https://doi.org/10.2352/ISSN.2470-1173.2021.9.IQSP-265

No-reference Image Quality Assessment of Underwater Images Using Multi-Scale Salient Local Binary Patterns

Muhammad Irshad[1], Camilo Sanchez-Ferreira[2], Sana Alamgeer[1], Carlos H. Llanos[3], and Mylène C.Q. Farias[1]

[1]Department of Electrical Engineering, University of Brasília, Brazil.
[2]Department of Physics, University of Cauca, Colombia.
[3]Department of Mechanical Engineering, University of Brasília, Brazil.

Abstract

Images acquired in underwater scenarios may contain severe distortions due to light absorption and scattering, color distortion, poor visibility, and contrast reduction. Because of these degradations, researchers have proposed several algorithms to restore or enhance underwater images. One way to assess these algorithms' performance is to measure the quality of the restored/enhanced underwater images. Unfortunately, since reference (pristine) images are often not available, designing no-reference (blind) image quality metrics for this type of scenario is still a challenge. In fact, although the area of image quality has evolved a lot in the last decades, estimating the quality of enhanced and restored images is still an open problem. In this work, we present a no-reference image quality evaluation metric for enhanced underwater images (NR-UWIQA) that uses an adapted version of the multi-scale salient local binary pattern operator to extract image features and a machine learning approach to predict quality. The proposed metric was tested on the UID-LEIA database and presented good accuracy performance when compared to other state-of-the-art methods. In summary, the proposed NR-UWQIA method can be used to evaluate the results of restoration techniques quickly and efficiently, opening a new perspective in the area of underwater image restoration and quality assessment.

Keywords: Underwater image enhancement; Image quality assessment; Quality metrics, full-reference, no-reference; Underwater image formation model; Saliency; Multiscale Salient Local Binary Patterns;

Introduction

Underwater images are often characterized by a poor visibility since the light travelling in the water medium is attenuated and, consequently, the captured scenes may be poorly contrasted and hazy. More specifically, light attenuation is produced by absorption and scattering processes. Absorption removes the light energy while scattering changes the direction of the light. Therefore, underwater images may have different types of degradations, including limited-range visibility, non-uniform lightening, low contrast, blurring, diminished color, bright artifacts, and noise. In other words, the visual aspect of underwater images may vary a lot depending on the water medium's characteristics, including the types of particles present in the water and the water depth [26]. Figure 1 shows examples of images captured underwater in three different scenarios: shallow water, deep water, and muddy water. Notice that, generally, degradations of images captured underwater are stronger than degradations of images captured over-the-air [39]. Often the quality of underwater images is not adequate for the to be used by image and computer vision algorithms, requiring the use of restoration or enhacement algorithms [39].

Given the importance of the overall quality of underwater-captured images for ocean engineering and scientific research, there are in the literature several methods for restoring or enhancing the quality of underwater images [16, 19]. Therefore, the use of underwater images in computer vision and image processing applications often depends on the success restoration and enhancement algorithms [35, 3, 15]. To determine the performance of these algorithms, we must estimate the quality of the restored/enhanced images as perceived by human viewers. Unfortunately, most methods used to estimate the performance of these algorithms do not consider human perception or image quality. One of the reasons is that subjective quality experiments, which are considered as the ground truth in image quality research, are costly and time-consuming [21]. Moreover, these methods are unfeasible for real-time applications and system integration. One viable option to estimate the quality of restored or enhanced underwater images and, therefore, the restoration algorithm's performance is to use objective image quality assessment (IQA) methods.

IQA methods are algorithms capable of automatically estimate the quality of an image. These methods can be divided into three classes: (a) full-reference (FR) IQA methods, where a reference image is needed to estimate the quality; (2) reduced reference (RR) IQA methods, where partial information about the reference image is available; or (3) no-reference (NR) IQA methods, which blindly estimate quality without having access to the reference or pristine image. For underwater images scenario, where a reference image is not available, we must use NR-IQA methods to estimate the perceptual quality of restored and degraded images. IQA methods can be used to evaluate the restoration process's success and determine if the images are adequate for the target underwater engineering and monitoring applications. So far, a few researchers have proposed IQA methods specifically for underwater images. For example, Sanchez *et al.* [37] have proposed a restoration algorithm for underwater that uses an NR-IQA method as a performance metric for the optimization algorithm.

Although in the last decades a lot of progress has been made in the area of image quality assessment, designing metrics to estimate the quality of enhanced and restored images remains a challenge [8]. As mentioned earlier, the final quality of underwater images depend on the marine habitats where the images are captured, which often introduce specific chroma, saturation, and contrast degradations [45, 43]. Therefore, it is important to develop dedicated image quality assessment methods for underwater scenarios. So far, few blind (no-reference) image quality metrics have been proposed with the goal of evaluating the quality of underwater images [34].

In this work, we propose a no-reference (underwater) image quality assessment (NR-UWIQA) method. More specifically, the proposed NR-IQA method is targeted at restored underwater images and uses a multi-scale salient local binary patterns operator [13]. The NR-UWIQA method is able to identify the quality differences in both distorted and restored/enhanced underwater images, producing quality scores that are well correlated with subjective quality scores provided by human viewers. To achieve this, we have adapted a modified version of the Multiscale Salient Local Binary Patterns (MSLBP) [14] that is a no-reference IQA based on machine learning. The final results on underwater images show that the proposed method performs better than other state-of-the-art metrics. Additionally, the NR-UWIQA has a low computational complexity and can be implemented in real-time.

This paper is divided as follows. First, we discuss the underwater image formation model. Then, we describe currently available underwater image quality assessment methodologies. Then, we detail the proposed methodology, present the experimental results and our conclusions.

Figure 1: Examples of images acquired underwater under different conditions: shallow water (left), deep water (center), and muddy water(right). These images are taken from AQUALOC dataset [11].

Underwater Image Formation Model

While being transmitted through the water medium, light is attenuated by either absorption or scattering. In absorption, the interactions of the light with the medium matter along the propagation path cause the attenuation. So, absorption may cause a significant loss of the image brightness and, depending on the wavelength and the object distance, color distortions [6, 7]. Scattering corresponds to a change of the light direction caused by the collision of photons and particles in the water. There are two types of scattering: (a) *back-scattering*, in which a fraction of the light reflected by the water particles is captured by the camera before reaching the objects, therefore reducing the image contrast and (sometimes) creating bright spots, and (b) *forward-scattering* in which the light changes direction along the path between the object and the camera, introducing blurring [38].

There are several models that aim to characterize underwater light propagation, with the most popular and complete physical model being the model proposed by Jaffe-McGlamery [28, 22]. Figure 2 illustrates the fundamentals of this model, where the light captured in the underwater medium is represented as the linear superposition of a direct component, a forward component, and a back scatter component. These three components are linearly

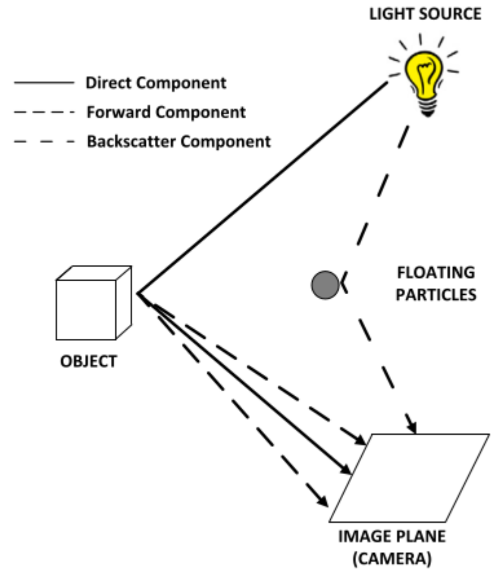

Figure 2: Illustration of the Jaffe-McGlamery model for underwater light propagation [37].

combined to compose the irradiance, as given by the following equation:

$$E_t = E_d + E_f + E_b, \tag{1}$$

where E_t is the total irradiance, E_d is the direct component, E_f is the forward component, and E_b is the back scatter component.

Jaffe-McGlamery also proposed a simplified model in which the light intensity is exponentially reduced as it travels through the water medium, as given by the following equation [42]:

$$E_i(d) = E_{0,i} \cdot e^{-C_i \cdot d}, \tag{2}$$

where $E_i(d)$ is the light intensity of a wavelength i at a distance d, $E_{0,i}$ is the light intensity of a wavelength i at the light source, and C_i is the attenuation coefficient for wavelength i. Note that the attenuation coefficient depends on the wavelength of the light or, in other words, of the light color [25] that leads to the strong color distortions presented in underwater images.

Underwater Image Quality Assessment (IQA) methods

Currently, there are many general-purpose IQA methods [8, 23]. Example of simple and popular IQA methods are the mean square error (MSE), the peak-to-signal noise ratio (PSNR), and the structural similarity measure (SSIM) [40]. There are also specific quality metrics that aim to measure a certain aspect of image quality. For example, the Underwater Colour Image Quality Evaluation (UCIQE) [45] metric that quantifies the non-uniform color cast, blurring, and low-contrast characteristics of underwater images for quality assessment. The Patch-based mean Underwater Image Quality (PUIQ) [43] metric incorporates log-contrast power spectrum features of underwater images. However, currently available IQA methods have shown little success when evaluating the quality of underwater images. It is worth pointing out that in underwater environments, pristine or undegraded images are usually unavailable and, therefore, NR-IQA methods are the only viable approach for these applications.

Among the few IQA methods specially designed for underwater applications is the metric proposed by Panette *et al.* - the underwater image quality measure (UIQM) [34]. UIQM is a NR-IQA method that explores the three-dimensional contrast measure relationship of RGB color channels. CRME [33] is a metric that measures the color differences between a center pixel and its neighbouring pixels for quality assessment. Hou *et al.* [20] proposed an IQA metric for scattered-blurred underwater images, which is based on a weighted gray scale angle (WGSA). Arredondo *et al.* [4] proposed an IQA method to measure the robustness of the algorithms to underwater noise. Yang *et al.* [44] proposed an underwater IQA metric based on the log-contrast power spectrum and on a perceptual sharpness metric.

In underwater image processing, many researches have used different types of objective methods to evaluate the performance of their techniques. For example, Chiang *et al.* [9] applied signal-to-noise ratio (SNR) and MSE to estimate the performance of their proposed method. Pramunendar *et al.* [36] analyzed the performance of their method by computing the number of matching points with a SIFT registration process.

Proposed Methodology

To assess the quality of underwater images, we have used a blind image quality assessment (NR-IQA) method named the Multiscale Salient Local Binary Patterns (MSLBP) [14]. The MSLBP is based on machine learning algorithm and does not use any information from the reference source content. This method uses an extension of the multiscale local binary pattern (MLBP) algorithm [12], which is a variant of the local binary pattern (LBP) [31], to extract features that are relevant to image quality.

The LBP operator can be computed using the following equation:

$$L_R^P(\mathscr{I}_c) = \sum_{p=0}^{P-1} \sigma(\mathscr{I}_p, \mathscr{I}_c) 2^p, \tag{3}$$

where $\mathscr{I}$ is an input image, $\mathscr{I}_c = \mathscr{I}(x,y)$ is arbitrary central pixel at the position (x,y), $\mathscr{I}_p = \mathscr{I}(x_p, y_p)$ is a neighboring pixel surrounding $\mathscr{I}_c$, and $\sigma(u,v)$ is the step function given by:

$$\sigma(v,u) = \begin{cases} 1, & \text{if } v-u \geq 0, \\ 0, & \text{otherwise.} \end{cases} \tag{4}$$

The points (x,y) are related to the neighboring points (x_p, y_p) as follows:

$$x_p = x + R\cos\left(2\pi \frac{p}{P}\right) \quad \text{and} \quad y_p = y - R\sin\left(2\pi \frac{p}{P}\right).$$

In the above equations, $p = \{1, 2, \cdots, P\}$ is the number of neighboring pixels sampled from a distance of R from $\mathscr{I}_c$ to $\mathscr{I}_p$. Figure 3 describes the steps for applying the LBP operator on a single pixel ($\mathscr{I}_c = 8$) located in the center of a 3×3 image block, as shown in the bottom-left of this figure. The numbers in the gray squares of the block represent the order in which the operator is computed (clockwise direction, starting from 0). In this figure, we use a unitary neighborhood radius ($R = 1$) and eight neighboring pixels ($P = 8$).

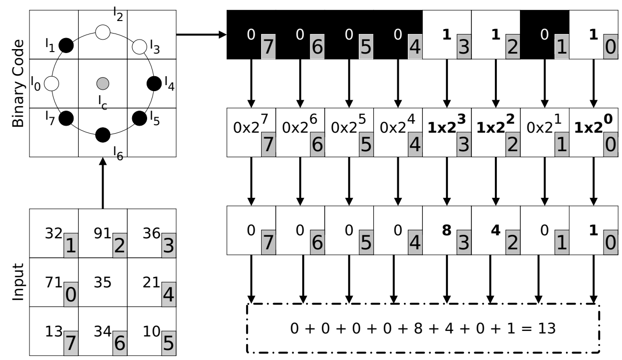

Figure 3: Example of LBP algorithm using $R = 1$, $P = 8$, $\mathscr{I}_c = 35$, $\mathscr{I}_p = \{71, 32, 91, 103, 21, 10, 34, 13\}$, and $L_1^8(35) = 13$ [12].

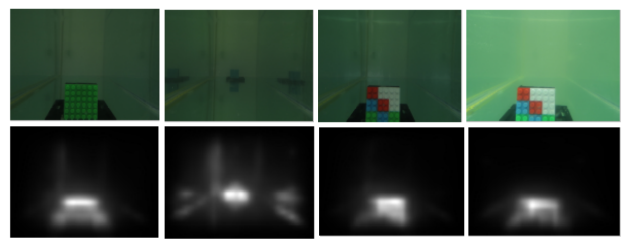

Figure 4: underwater images and their salient maps.

After calculating $\sigma(v,u)$ for each neighboring pixel $\mathscr{I}_p$, we obtain a binary output for each $\mathscr{I}_p$ ($0 \leq p \leq 7$), as illustrated in the block in the upper-left position of Figure 3. In this block, black circles correspond to "0" and white circles to "1". These binary outputs are stored in a binary format, according to their position (gray squares). Then, the resulting binary number is converted to the decimal format. This decimal number is the output produced by LBP for $\mathscr{I}_c$. Then, we compute the LBP labels for all pixels of an image, obtaining the LBP maps.

Instead of using single values for R, P, MLBP generates multiscale LBP maps by varying the parameters R and P and performing a symmetrical sampling. For a set of parameters R and P, the MLBP operator computes the LBP labels of all pixels in an image and obtains a set of LBP maps ($\mathscr{L}_R^P$). In MSLBP, the spatial features extracted by the MLBP operator are weighted by a saliency map generated by a Boolean Map saliency model (BMS) [46]. BMS saliency maps $\mathscr{W}(x,y)$ have values between 1 and 0, which represent the salience value of the corresponding pixel in the underwater image. We name each weighted map as the salient local binary pattern (SLBP) map, while the weighted maps of the MLBP maps are named multiscale SLBP (MSLBP) maps. The weighted features computed for the MSLBP are used as input to a supervised machine learning algorithm that predicts the final image quality score.

In this work, instead of using the BMS algorithm, we use the Graph-Based Visual Saliency (GBVS) [17] model to generate the saliency maps $\mathscr{W}$. Figure 4 shows samples of saliency maps generated by the GBVS model using a few underwater images as input images. We chose the GBVS model because it is a traditional model that is easy to execute and it has a similar performance to the BMS model proposed in the original MSLBP method [14]. The saliency maps $\mathscr{W}$ are used weigh each pixel of the MLBP maps $\mathscr{L}_R^P$. A feature vector is obtained by computing the histogram of the $\mathscr{L}_R^P$ maps weighted by the salience maps $\mathscr{W}$. Particularly, the histogram is generated as:

$$H_R^P = \{h_R^P(0), h_R^P(1), \cdots, h_R^P(P+1)\} \tag{5}$$

where:

$$h_R^P(\phi) = \sum_{x,y} \mathscr{W}(x,y) \cdot \delta(\mathscr{L}_R^P(x,y), \phi), \tag{6}$$

and

$$\delta(v,u) = \begin{cases} 1, & \text{if } v = u, \\ 0, & \text{otherwise.} \end{cases} \tag{7}$$

The number of bins of this histogram is similar to the number of different labels in $\mathscr{L}_R^P$. So, each $\mathscr{L}_R^P(i,j)$ can be represented by its weighted form, generating the map $\mathscr{S}_R^P$. Figures 5 (a) and (b) depict the examples of the input images and their saliency maps, respectively. Figures 5 (c) to (h) depict examples of LBP maps obtained using different radius values (R) and different numbers of neighboring points (P). Figures 5 (i) to (n) display the SLBP maps generated from $\mathscr{W}$ and their corresponding $\mathscr{L}_R^P$. In this work, we have used $R = 1, 2$, and 3 and $P = 4, 8$, and 16.

After generating the SLBP maps, we compute the different SLBP histograms H, as illustrated in Figure 6. These histograms are concatenated to produce a feature vector for each underwater image as:

$$\mathscr{H} = H_1^4 \oplus H_1^8 \oplus H_2^4 \oplus H_2^8 \oplus H_2^{16} \oplus \cdots \oplus H_R^N, \tag{8}$$

where $\oplus$ denotes the concatenation operator.

The computed feature vector $\mathscr{H}$ is supplied as input to a random forests (RFR) regression algorithm to predict the quality of underwater images. We chose RFR because in previous studies it has shown robust performance values [10] when compared to other machine learning algorithms (e.g. neural networks, support vector machines, generalized linear models, etc.).

Underwater Image Quality databases

There are many real-world underwater image datasets. One example is the Fish4Knowledge dataset [18], which is used for target detection and recognition. The SUN dataset [41] is used for object detection, the MARIS dataset [27] is used for marine autonomous robotics, and the SEA-thru [2] dataset is used for range maps. However, existing datasets do not provide ground truth or reference images and, therefore, it is often difficult to design image quality metrics for this type of applications. Recently, Sanchez *et al.* proposed the UID-LEIA (Underwater Image Database of Laboratory of Embedded Systems and Integrated circuits Applications) dataset [37]. Figures 5-7 all shows examples of underwater images from the UID-LEIA dataset. Figure 7 shows a sample of the 45 reference images and 135 distorted underwater images contained in this dataset. Besides the images, UID-LEIA also contains subjective quality scores for all these images, which makes it possible to use this dataset in the design of underwater IQA methods.

Experimental Setup and Results

In this work, we use the UID-LEIA database for training and testing the proposed underwater IQA metric. We used the Spearman's Rank Order Correlation Coefficient (SROCC), Pearson's Linear Correlation Coefficient (PLCC), the Kendall Rank Correlation (KRCC), and Root Mean Square Error (RMSE) as performance metrics. We compare the proposed methods with the following publicly available underwater IQA methods: the Underwater Colour Image Quality Evaluation (UCIQE) [45] and the Patch-based mean Underwater Image Quality (PUIQ) [43]. Additionally, we also compare our method with traditional NR-IQA methods: CORNIA [32], BRIQUE [1], SSEQ [24], DIIVINE [30], NIQE [29], Choi *et al.* [47], and Balboa *et al.* [5]. The experiments were performed on using a PC with an Intel Core i7-4790 processor at 3.60GHz, running an Ubuntu operating system. From the UID-LEIA dataset, 80% of the content is used for training and 20% is used for testing. This 80-20 training-testing random split is performed 1,000 times and then the mean correlation is computed and reported.

Table 1 illustrates the performance comparison of proposed method with other state-of-the art metrics on the UID-LEIA dataset. Notice that the proposed metric outperforms all other metrics with respect to SROCC, PLCC and RMSE values. The highest KRCC values are obtained by NIQE metric. The values in bold correspond to the best performance, while the results in italics correspond to the second best results. These results show the superiority of the proposed approach in terms of accuracy, monotonicity and consistency.

Table 1: Performance evaluation of proposed method with different IQA methods on UID-LEIA dataset.

Type	Method	KRCC	PLCC	SROCC	RMSE
NR-IQA Methods	CORNIA	0.6502	0.4549	0.6394	32.1954
	SSEQ	0.0247	0.0129	0.0199	35.7431
	BRISQUE	0.1719	0.0998	0.1688	27.2345
	DIIVINE	0.7038	0.5724	0.6958	25.5244
	NIQE	**0.9372**	*0.7258*	*0.9357*	*11.5852*
	Choi *et al.* [47]	0.6900	0.4679	0.6867	31.9258
	Balboa *et al.* [5]	0.3958	0.2486	0.4138	35.2584
NR-IQA Methods for Underwater Images	UCIQE	*0.9005*	0.6854	0.8992	16.1584
	PUIQ	0.5968	0.3589	0.6002	33.4852
	Proposed	0.8286	**0.9502**	**0.9475**	**8.4735**

Conclusions

In this work, we have adapted a no-reference multiscale salient local binary pattern method to assess the visual quality of underwater images. Result suggest that the proposed metric is efficient and fast and can be implemented in real-time for different underwater image quality applications. The main contribution of this work is the design of a specific NR-UWIQA method that can be used in underwater enhancement and restoration application. The proposed metric is simple and fast, achieving good and robust results.

Acknowledgments

This work has been supported by the Federal District Research Support Foundation (FAP-DF), Brazil, by the Coordenação de Aperfeiçoamento de Pessoal de Nível Superior (CAPES), and by the University of Brasilia (UnB), Brasilia, Brazil.

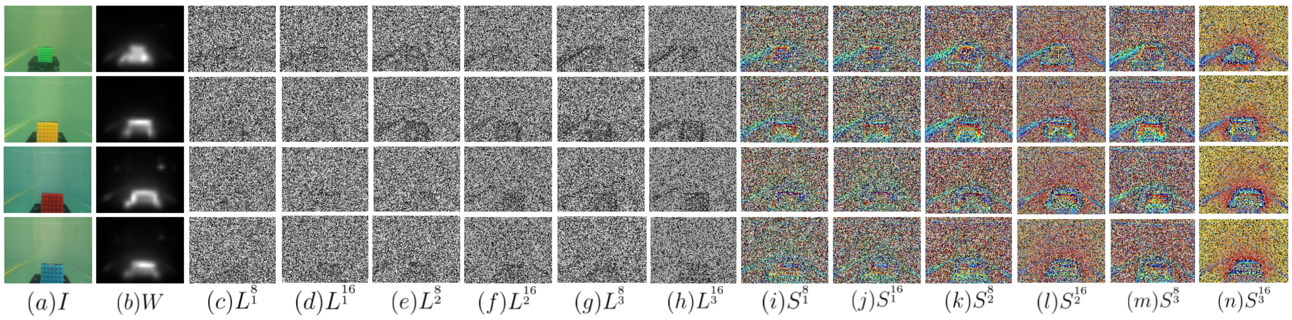

Figure 5: Example of underwater images (a), their saliency maps (b), LBP maps (c)-(h), and SLBP maps (i)-(n).

References

[1] A. Mittal, A. K. M., and Bovik, A. C. No-reference image quality assessment in the spatial domain. *IEEE Transactions on Image Processing* (2012).

[2] Akkaynak, D., and Treibitz, T. Sea-thru: A method for removing water from underwater images. In *Proceedings of the IEEE conference on computer vision and pattern recognition* (2019), pp. 1682–1691.

[3] Ancuti, C. O., Ancuti, C., De Vleeschouwer, C., and Bekaert, P. Color balance and fusion for underwater image enhancement. *IEEE Transactions on image processing 27*, 1 (2017), 379–393.

[4] Arredondo, M., and Lebart, K. A methodology for the systematic assessment of underwater video processing algorithms. In *Europe Oceans 2005* (2005), vol. 1, IEEE, pp. 362–367.

[5] Balboa, R. M., and Grzywacz, N. M. Occlusions and their relationship with the distribution of contrasts in natural images. *Vision Research 40*, 19 (2000), 2661 – 2669.

[6] Barros, W. F. *Uma Abordagem Automática para Restauração de Imagens de Cenas Subaquáticas*. PhD thesis, Federal University of Minas Gerais (UFMG), Belo Horizonte - Brazil, 2010.

[7] Bazeille, S., Quidu, I., and Jaulin, L. Color-based underwater object recognition using water light attenuation. *Journal of Intelligent Service Robotics 5*, 2 (2012), 109–118.

[8] Chandler, D. M. Seven challenges in image quality assessment: past, present, and future research. *ISRN Signal Processing 2013* (2013).

[9] Chiang, J. Y., and Chen, Y.-C. Underwater image enhancement by wavelength compensation and dehazing. *IEEE Transactions on Image Processing 21*, 4 (2011), 1756–1769.

[10] Fernández-Delgado, M., Cernadas, E., Barro, S., and Amorim, D. Do we need hundreds of classifiers to solve real world classification problems. *Journal of Machine Learning Research 15*, 1 (2014), 3133–3181.

[11] Ferrera, M., Creuze, V., Moras, J., and Trouvé-Peloux, P. Aqualoc: An underwater dataset for visual–inertial–pressure localization. *The International Journal of Robotics Research 38*, 14 (2019), 1549–1559.

[12] Freitas, P. G., Akamine, W. Y., and Farias, M. C. Blind image quality assessment using multiscale local binary patterns. *Journal of Imaging Science and Technology 60*, 6 (2016), 60405–1.

[13] Freitas, P. G., Alamgeer, S., Akamine, W. Y., and Farias, M. C. Blind image quality assessment based on multiscale salient local binary patterns. In *Proceedings of the 9th ACM Multimedia Systems Conference* (2018), pp. 52–63.

[14] Freitas, P. G., Alamgeer, S., Akamine, W. Y. L., and Farias, M. C. Q. Blind image quality assessment based on multiscale salient local binary patterns. MMSys '18, Association for Computing Machinery, p. 52–63.

[15] Ghani, A. S. A., and Isa, N. A. M. Underwater image quality enhancement through integrated color model with rayleigh distribution. *Applied soft computing 27* (2015), 219–230.

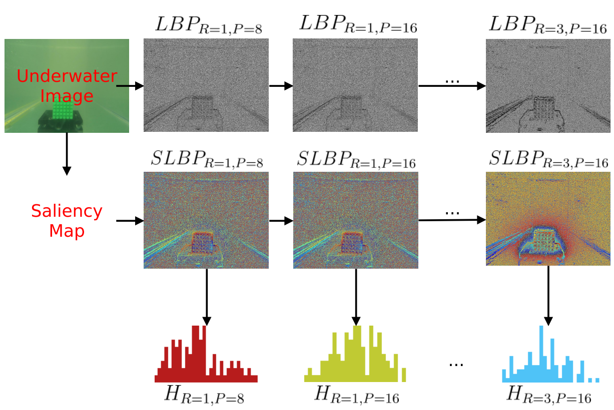

Figure 6: Multiple histogram generation from SLBP.

Figure 7: Underwater images from UID-LEIA database

[16] HAN, F., YAO, J., ZHU, H., AND WANG, C. Underwater image processing and object detection based on deep cnn method. *Journal of Sensors 2020* (2020).

[17] HAREL, J., KOCH, C., AND PERONA, P. Graph-based visual saliency. In *Proceedings of the 19th International Conference on Neural Information Processing Systems* (Cambridge, MA, USA, 2006), NIPS'06, MIT Press, pp. 545–552.

[18] HE, J., VAN OSSENBRUGGEN, J., AND DE VRIES, A. Fish4label: accomplishing an expert task without expert knowledge. pp. 211–212.

[19] HOU, W., GRAY, D. J., WEIDEMANN, A. D., FOURNIER, G. R., AND FORAND, J. Automated underwater image restoration and retrieval of related optical properties. In *2007 IEEE International Geoscience and Remote Sensing Symposium* (2007), IEEE, pp. 1889–1892.

[20] HOU, W., WEIDEMANN, A. D., GRAY, D. J., AND FOURNIER, G. R. Imagery-derived modulation transfer function and its applications for underwater imaging. In *Applications of Digital Image Processing XXX* (2007), vol. 6696, International Society for Optics and Photonics, p. 669622.

[21] ITU-R. Recommendation 500-11: Methodology for the Subjective Assessment of the Quality of Television Pictures. *Int. Telecomm. Union, Geneva* (2002).

[22] JAFFE, J. S. Computer modeling and the design of optimal underwater imaging systems. *IEEE Journal of Oceanic Engineering 15*, 2 (1990), 101–111.

[23] KEELAN, B. W. Objective and subjective measurement and modeling of image quality: a case study. In *Applications of Digital Image Processing XXXIII* (2010), vol. 7798, International Society for Optics and Photonics, p. 779815.

[24] L. LIU, B. LIU, H. H., AND BOVIK, A. No-reference image quality assessment based on spatial and spectral entropies. *Signal Processing: Image Communication* (June 2014).

[25] LEE, D., KIM, G., KIM, D., MYUNG, H., AND CHOI, H.-T. Vision-based object detection and tracking for autonomous navigation of underwater robots. *Ocean Engineering 48* (2012), 59–68.

[26] M UPLAVIKAR, P., WU, Z., AND WANG, Z. All-in-one underwater image enhancement using domain-adversarial learning. In *The IEEE Conference on Computer Vision and Pattern Recognition (CVPR) Workshops* (June 2019).

[27] (MARIS), T. I. M. I. S. The marine information system, may 2019.

[28] MCGLAMERY, B. A computer model for underwater camera systems. In *Ocean Optics VI* (1980), vol. 208, International Society for Optics and Photonics, pp. 221–231.

[29] MITTAL, A., SOUNDARARAJAN, R., AND BOVIK, A. C. Making a "completely blind" image quality analyzer. *IEEE Signal Processing Letters 20*, 3 (2013), 209–212.

[30] MOORTHY, A. K., AND BOVIK, A. C. Blind image quality assessment: From scene statistics to perceptual quality. *EEE Transactions Image Processing* (December 2011), 3350–3364.

[31] OJALA, T., PIETIKÄINEN, M., AND MÄENPÄÄ, T. Multiresolution gray-scale and rotation invariant texture classification with local binary patterns. *IEEE Trans. Pattern Anal. Mach. Intell. 24* (2002), 971–987.

[32] P. YE, J. KUMAR, L. K., AND DOERMANN, D. Unsupervised feature learning framework for no-reference image quality assessment. *IEEE Conference on Computer Vision and Pattern Recognition (CVPR)* (2012).

[33] PANETTA, K., GAO, C., AND AGAIAN, S. No reference color image contrast and quality measures. *IEEE transactions on Consumer Electronics 59*, 3 (2013), 643–651.

[34] PANETTA, K., GAO, C., AND AGAIAN, S. Human-visual-system-inspired underwater image quality measures. *IEEE Journal of Oceanic Engineering 41*, 3 (2015), 541–551.

[35] PENG, Y.-T., AND COSMAN, P. C. Underwater image restoration based on image blurriness and light absorption. *IEEE transactions on image processing 26*, 4 (2017), 1579–1594.

[36] PRAMUNENDAR, R. A., SHIDIK, G. F., SUPRIYANTO, C., ANDONO, P. N., AND HARIADI, M. Auto level color correction for underwater image matching optimization. *Int. J. Comput. Sci. Netw. Secur. 13*, 1 (2013), 18–23.

[37] SÁNCHEZ-FERREIRA, C., COELHO, L., AYALA, H. V., FARIAS, M. C., AND LLANOS, C. H. Bio-inspired optimization algorithms for real underwater image restoration. *Signal Processing: Image Communication 77* (2019), 49–65.

[38] SCHETTINI, R., AND CORCH, S. Underwater image processing: State of the art of restoration and image enhancement methods. *EURASIP Journal on Advances in Signal Processing* (2010), 1–14.

[39] SCHETTINI, R., AND CORCHS, S. Underwater image processing: state of the art of restoration and image enhancement methods. *EURASIP Journal on Advances in Signal Processing 2010* (2010), 1–14.

[40] WANG, Z., BOVIK, A. C., SHEIKH, H. R., AND SIMONCELLI, E. P. Image quality assessment: from error visibility to structural similarity. *IEEE transactions on image processing 13*, 4 (2004), 600–612.

[41] XIAO, J., EHINGER, K. A., HAYS, J., TORRALBA, A., AND OLIVA, A. Sun database: Exploring a large collection of scene categories. *Int. J. Comput. Vision 119*, 1 (Aug. 2016), 3–22.

[42] YAMASHITA, A., FUJII, M., AND KANEKO, T. Color registration of underwater images for underwater sensing with consideration of light attenuation. In *Proceedings 2007 IEEE International Conference on Robotics and Automation* (2007), IEEE, pp. 4570–4575.

[43] YANG, M., AND SOWMYA, A. New image quality evaluation metric for underwater video. *Signal Processing Letters, IEEE 21* (10 2014), 1215–1219.

[44] YANG, M., AND SOWMYA, A. New image quality evaluation metric for underwater video. *IEEE Signal Processing Letters 21*, 10 (2014), 1215–1219.

[45] YANG, M., AND SOWMYA, A. An underwater color image quality evaluation metric. *IEEE Transactions on Image Processing 24*, 12 (2015), 6062–6071.

[46] ZHANG, J., AND SCLAROFF, S. Exploiting surroundedness for saliency detection: a boolean map approach. *IEEE transactions on pattern analysis and machine intelligence 38*, 5 (2016), 889–902.

[47] ZHOU, Y., LI, L., WANG, S., JINJIAN, W., FANG, Y., AND GAO, X. No-reference quality assessment for view synthesis using dog-based edge statistics and texture naturalness. *IEEE Transactions on Image Processing PP* (04 2019), 1–1.

Author Biography

Muhammad Irshad *received his B.Sc degree in computer science form Bahauddin Zakariya University, Multan, Pakistan in 2009 and M.S. degree in computer science from Air University Islamabad, Pakistan, in 2015. Currently, he is a Ph.D. candidate in the Electronic Engineering and System Automation program of the University of Brasília, Brasília, Brazil. His research interests include image and video quality assessment, multimedia contents and machine learning.*

Camilo Sanchez-Ferreira *received the B.Sc. degree in physics engineering from the University of Cauca, Colombia, in 2008, the M.Sc. and Ph.D. degrees in Mechatronics Systems from the University of Brasilia, in 2012 and 2017, respectively. He is currently Professor with the Department of Physics at University of Cauca. His research interests include Image Processing and Computer Vision, automation and control, instrumentation and artificial intelligent systems.*

Sana Alamgeer *received her B.Sc degree in computer science from Bahauddin Zakariya University, Multan, Pakistan in 2009 and M.S. degree in computer science from Air University Islamabad, Pakistan, in 2015. Currently, she is a Ph.D. candidate in the electrical engineering and system automation program at University of Brasília, Brazil. She is a researcher at the Group of Digital Signal Processing (GPDS) and her current interests include image / video quality metrics, visual attention, Light Field image processing and deep learning.*

Carlos H. Llanos *received the B.Sc. degree in electrical engineering from the Universidad del Valle, Colombia, in 1983, the M.Sc. degree in computer science from the Universidade Federal de Minas Gerais, in 1990, and the Ph.D. degree in electrical engineering from the Universidade de São Paulo, in 1998. He is currently an Associate Professor with the Department of Mechanical Engineering, Universidade de Brasília, where he is also the Leader of the Automation and Control Group (GRACO). His research interests include reconfigurable systems, automation and control, automatic systems synthesis, instrumentation, building and home automation, and intelligent systems. Dr. Llanos is member of IEEE.*

Mylene C. Q. Farias *received her B.Sc. degree in electrical engineering from Federal University of Pernambuco (UFPE), Brazil, in 1995 and her M.Sc. degree in electrical engineering from the State University of Campinas (UNICAMP), Brazil, in 1998. She received her Ph.D. in electrical and computer engineering from the University of California Santa Barbara (UCSB), USA, in 2004 for work in no-reference video quality metrics. Dr. Farias has worked as a research engineer at CPqD (Brazil) in video quality assessment and validation of video quality metrics. She has also worked as an intern for Philips Research Laboratories (The Netherlands) in video quality assessment of sharpness algorithms and for Intel Corporation (Phoenix, USA) developing no-reference video quality metrics. Currently, she is an Associate professor in the Department of Electrical Engineering at the University of Brasilia (UnB). Her current interests include video quality metrics, video processing, multimedia signal processing, watermarking, and visual attention. Dr. Farias is a member of IEEE, the IEEE Signal Processing Society, ACM, and SPIE*